Manuscript Details

Manuscript number	CCC_2018_454_R1
Title	INFLUENCE OF THE ALKALINE SOLUTION AND TEMPERATURE ON THE RHEOLOGY AND REACTIVITY OF ALKALI-ACTIVATED FLY ASH PASTES
Article type	Research Paper

Abstract

The aim of the present research is to ascertain the effect of the nature and concentration of the alkaline activator and temperature on the rheological behaviour of alkali-activated fly ash (AAFA) pastes. Furthermore, the reaction process of fly ash has been investigated from rheological measurements. Results have shown that the increase of the activator concentration and the temperature leads to an increase of yield stress and apparent viscosity, mainly at temperatures above 65 oC when dissolution of fly ash and precipitation of hydration products is raised. In general, similar activation energies were determined for alkaline-activated fly ash pastes, regardless of the concentration and silica modulus of the activator, concluding that the underlying reaction mechanism is the same independently on the nature of the activating solution.

Keywords	alkali-activated fly ash, rheology, activation energy, temperature, alkaline activator

Corresponding Author	Marta Palacios
Corresponding Author's Institution	CSIC
Order of Authors	Marta Palacios, Maria del Mar Alonso, Varga Celia, Francisca Puertas

Submission Files Included in this PDF

File Name [File Type]

Reviewers comments.docx [Response to Reviewers]

Rheology of AAFA_R1_F.docx [Revised Manuscript with Changes Marked]

Rheology of AAFA_F.docx [Manuscript File]

To view all the submission files, including those not included in the PDF, click on the manuscript title on your EVISE Homepage, then click 'Download zip file'.

INFLUENCE OF THE ALKALINE SOLUTION AND TEMPERATURE ON THE RHEOLOGY AND REACTIVITY OF ALKALI-ACTIVATED FLY ASH PASTES

M. Palacios*, M. M. Alonso, C. Varga, F. Puertas

Eduardo Torroja Institute for Construction Sciences (IETcc-CSIC), Madrid (Spain)

*Corresponding author: Dr. Marta Palacios (marta.palacios@ietcc.csic.es)

Abstract

The aim of the present research is to ascertain the effect of the nature and concentration of the alkaline activator and temperature on the rheological behaviour of alkali-activated fly ash (AAFA) pastes. Furthermore, the reaction process of fly ash has been investigated from rheological measurements.

Results have shown that the increase of the activator concentration and the temperature leads to an increase of yield stress and apparent viscosity, mainly at temperatures above 65 ºC when dissolution of fly ash and precipitation of hydration products is raised. In general, similar activation energies were determined for alkali-activated fly ash pastes, regardless of the concentration and silica modulus of the activator, concluding that the underlying reaction mechanism is the same independently on the nature of the activating solution.

Keywords: alkali-activated fly ash, rheology, activation energy, temperature, alkaline activator

1.-INTRODUCTION

An understanding and control of the rheological properties of cementitious materials is essential to ascertain their optima mixing, handling and casting as well as strength and durability after hardening [1-3]. It is well-known that the rheological behaviour of cementitious materials is affected by several parameters such as mixing conditions (energy, time or temperature), cement mineralogical composition, supplementary cementitious materials (SCMs), chemical admixtures, water/cement ratio, solid particle size distribution and aggregate content and morphology [1, 2, 4-14].

Rheological behaviour of Portland cement-based materials has been widely studied, however, very few studies have been performed on alkali-activated materials (AAMs). An understanding and control of the rheology of such materials are essential to establish the manufacturing criteria to be laid down in standards governing their use as binders and to ultimately bring these eco-efficient construction materials to market.

Previous studies have confirmed the crucial role of the alkaline solution on the rheology of AAMs. In particular, NaOH-activated slag (AAS) pastes behave as Bingham fluid [15, 16] while waterglass- AAS fit to Herschel-Bulkley model [15, 17]. Furthermore, when waterglass is used as activator, a rise of the SiO_2/Na_2O ratio decreases the fluidity of AAM suspensions [16, 18]. Torres-Carrasco et al. [19] have reported an improvement of the rheological behavior in pastes activated with waste glass solution compared to commercial waterglass, confirming the feasibility of using waste glass as an alternative activator from the rheological point of view. In any case, regardless of the activating

solution used, a decrease of the fluidity of AAMs with the increase of the activator concentration has been reported [16, 18].

AAMs reaction process has been extensively investigated by a broad number of techniques, concluding that mineralogical and chemical composition of the aluminosilicate source have a direct influence on the type of reaction products and microstructure. In general, three main stages are involved in the reaction of AAMs: (1) dissolution of the aluminosilicate source releasing $Si(OH)^{-}_{4}$ and $Al(OH)_4^-$ into solution; (2) formation of a continuous gel upon solution supersaturation; and (3) condensation of aluminates and silicates oligomers in solution forming a large network [20, 21]. Rheological measurements have been proved to be a useful tool to provide a further understanding of the reaction process in AAMs. By a combination of heteronuclear liquid-state Nuclear Magnetic Resonance (NMR) and rheological measurements, Favier et al. [20] concluded the formation of an initial Al rich gel (Si/Al ≤ 4.5) at the grain pseudo-contact points as the main responsible of the initial (first 15 minutes) increase of the macroscopic elastic modulus of metakaolin-based geopolymer. Moreover, after several hours the precipitation of an aluminosilicate phase was linked to the paste setting.

Poulesquen et al. [22] have confirmed from rheological measurements the faster reaction kinetics of metakaolin when it is activated with NaOH compare to KOH, although the structure formed with KOH is more rigid, forming larger oligomers or favoring the connectivity of the tetrahedral network [22]. Furthermore, these authors reported no influence of the alkaline activator on the mechanism of reaction of

metakaolin. In contrast, fly ash source plays a role on the activation energy of the reaction process. In particular, the ferric oxide content in the fly ash has been reported as a rate-determining reactant [23].

The relative importance of the factors involved in alkali-activated systems rheology has yet to been established. The present study aims to ascertain the effect of factors such as the nature and concentration of the alkaline activator and temperature on the rheological behaviour of alkali-activated fly ash (AAFA) pastes. Moreover, this study aims to determine the effect of these factors on the reaction process of fly ash from rheological measurements, in particular, from the evolution of the pastes viscosity over time.

2. EXPERIMENTAL

2.1 Materials

Table 1 shows the chemical composition of the fly ash used in this study determined by X-ray fluorescence. The particle size distribution of the fly ash dispersed in isopropanol was determined by laser diffraction (Sympatec Helos 12LA) [24]. Table 2 shows respectively 10, 50 and 90 % size cut-offs of the Spanish fly ash (FA).

Table 1. Chemical composition of Fly ash (FA) (LOI = loss on ignition)

Chemical composition (% wt)											
SiO_2	CaO	Al_2O_3	Fe_2O_3	MgO	SO_3	Na_2O	K_2O	TiO_2	P_2O_5	MnO	LOI
54.40	2.70	27.5	6.40	1.50	---	0.50	3.1	1.3	0.3	>0.1	2.10

Table 2. Main parameters obtained from particle size distribution of FA

D_{v10} (µm)	D_{v50} (µm)	D_{v90} (µm)
3.46	17.54	74.42

A commercial sodium silicate (Merck waterglass: SiO_2/Na_2O molar ratio = 3.37; density = 1.36 g/mL) and NaOH pellets (98 % purity - Panreac) were used for the preparation of the alkaline solutions.

Table 3 lists the labels and physical and chemical characteristics of the activating solutions used. OH^- concentration was measured by HCl titration [25]. The dynamic viscosity of the activating solutions was determined in a 1.13-mm diameter SCHOTT Geräte capillary viscometer, immersed in a thermostat-controlled silicone oil bath to ensure a constant temperature of 25 °C.

Table 3. Physical and chemical properties of the activator solutions. (% Wg is refered to the percentage of sodium silicate solution by weight of activating solution)

Sample	Activator	% wt Wg	SiO_2/Na_2O	Density (g/cm^3)	Viscosity (mPa · s)	$[OH^-]$ (M)
AAFAN8	**8-M NaOH**	0	---	1.27	6.4	7.5
AAFAN8Wg15		15	0.16	1.29	6.9	6.4
AAFAN8Wg25		25	0.27	1.31	7.3	6.2
AAFAN10	**10-M NaOH**	0	--	1.35	11.0	9.9
AAFAN10Wg15		15	0.13	1.35	11.6	8.1
AAFAN10Wg25		25	0.23	1.35	12.3	6.3

2.2 Sample preparation and tests conducted

2.2.1 Paste preparation

Alkali-activated fly ash (AAFA) pastes were prepared by mixing at room temperature 80 g of fly ash with 20 g of the alkaline solution (liquid/solid ratio = 0.25) for three minutes with a mechanical stirrer at 700 rpm. The alkaline solution was prepared by dissolving NaOH in water and adding afterwards the corresponding amount of Na_2SiO_3

solution. In all the experiments, the liquid/solid ratio (in mass) was kept constant. Rheological properties and fluidity of the pastes were subsequently tested as described below.

2.2.2. Rheological behavior

Three main rheological tests were performed:

(a) Yield stress evaluation from flow curves: AAFA pastes were placed in a Haake Rheowin Pro RV1 rotational viscometer fitted with a grooved Z38/S cylindrical rotor blade and a built-in Haake DC30-B3 water recirculation system for thermostatic control. Rate controlled measurements were performed according to the following steps: (1) initial pre-shearing at 100 s^{-1} for 30 seconds, (2) increase of the shear rate from 0 to 100 s^{-1} in 60 s, (3) decrease of the share rate from 100 to 0 s^{-1} in 90 s. These tests were run at temperatures in the range from 25 to 85 °C. The yield stress values were determined from the down-rate curves that satisfactory fit to Herschel-Bulkley model (Eq. 1).

$$\tau = \tau_0 + K \cdot \Upsilon^n \qquad \text{(Eq. 1)}$$

where τ is the shear stress, τ_o is yield stress (Pa), K is the consistency coefficient (Pa·s^n), γ is the shear rate and n is the dimensionless fluidity index.

(b) Fluidity loss over time: Minislump tests were performed to determine the fluidity of the AAFA pastes at 25, 65 and 85 °C over the first 30 minutes of reaction. Pastes were prepared by mixing 500 g of fly ash with 275g of the alkaline solution (l/s=0.55) by using an Ibertest Autotest 200/10 mixer. They were firstly mixed for 1.5 min at low speed (140 rpm) and after a 30-s pause, pastes were mixed for 1.5 min at high speed (285 rpm). Pastes were poured into a truncated conical mould (19 x 38.1 x

57.2 mm). The mould was afterwards removed from the samples that set on a flow table that was raised and dropped ten times. The diameter of the paste (Γ) was measured in the four directions and the average taken as the final value.

(c) Evolution of apparent viscosity at constant shear rate: The apparent viscosity of the AAFA pastes were tested for 30 minutes at a constant shear rate of 100 s^{-1} by using the Haake Rheometer Pro RV1 rotational viscosimeter described above. Measurements were performed at temperatures in the range between 25 and 85 °C. Apparent viscosity was determined as the shear stress applied to the suspension (measured by the viscosimeter) divided by the shear rate (Eq 2).

$$\mu = \frac{\tau}{\gamma} \qquad \text{(Eq. 2)}$$

3. RESULTS AND DISCUSSION

In the first part of this section, the impact of the nature and concentration of the activating solution and testing temperature on the rheological properties of AAFA pastes have been investigated. Afterwards, a deeper insight into the reaction process of fly ash was gained by evaluating the activation energy through rheological measurements.

3.1. Yield stress evaluation from flow curves

Figure 1 presents the hysteresis loops for the AAFA pastes activated with 8M and 10M NaOH, with and without addition of sodium silicate at 25 ºC, 65 ºC and 85 ºC. An increase of temperature involves an increment of the area of the hysteresis loop, inferring a greater structural breakdown. This is related to the enhance of the reactivity of the fly ash as temperature rises leading to greater interparticle bridges formed by the early hydration products [26].

A shear thinning behaviour is found for all the pastes bellow 100 s^{-1} and yield stress was determined by fitting the Herschel-Bulkey model in the range between 0.1 and 100 s^{-1}. From Figure 2, it is observed that at 25 ºC, the yield stress of suspensions activated with NaOH is higher compared to the waterglass-AAFA suspensions. It is well known that yield stress of a suspension depends on the viscosity of the fluid, interparticle forces and possible particle jamming [11, 18, 27]. Fraction of solids is similar in all the studied suspensions and consequently jamming will have a similar influence on their yield stress. NaOH solutions have a lower viscosity than waterglass solutions (see Table 3), that would not explain the greater yield stress values found in NaOH-AAFA. Therefore, different interparticle forces in NaOH- and waterglass- AAFA are the responsible of the different measured yield stress at 25 ºC. In particular, the adsorption of the silicates (from the waterglass solution) increases the overall negative surface charge of fly ash, increasing interparticle repulsive forces, leading to deflocculation of the particles and the lower yield stress for Wg-AAFA [28]. These results are in agreement with those found by Vance et al. [18]. In particular, these authors concluded a pseudo-Newtonian behaviour of NaOH- and KOH-activated AAFA pastes when waterglass was added to the solution.

Figure 2 also presents an increase of the yield stress with the increase of the temperature, mainly at temperatures equal or greater than 65 ºC when dissolution of fly ash and precipitation of hydration products is enhanced. In general, yield stress also increases with the rise of the solution concentration, as it accelerates fly ash reaction increasing the amount of percolated early hydration products [29]. Surprisingly, and with the exception of AAFAN10 and AAFAN8Wg15, similar yield stress values have been

measured for pastes cured at 75 °C and 85 °C. This could be due to possible artefacts during the experiments at high temperature.

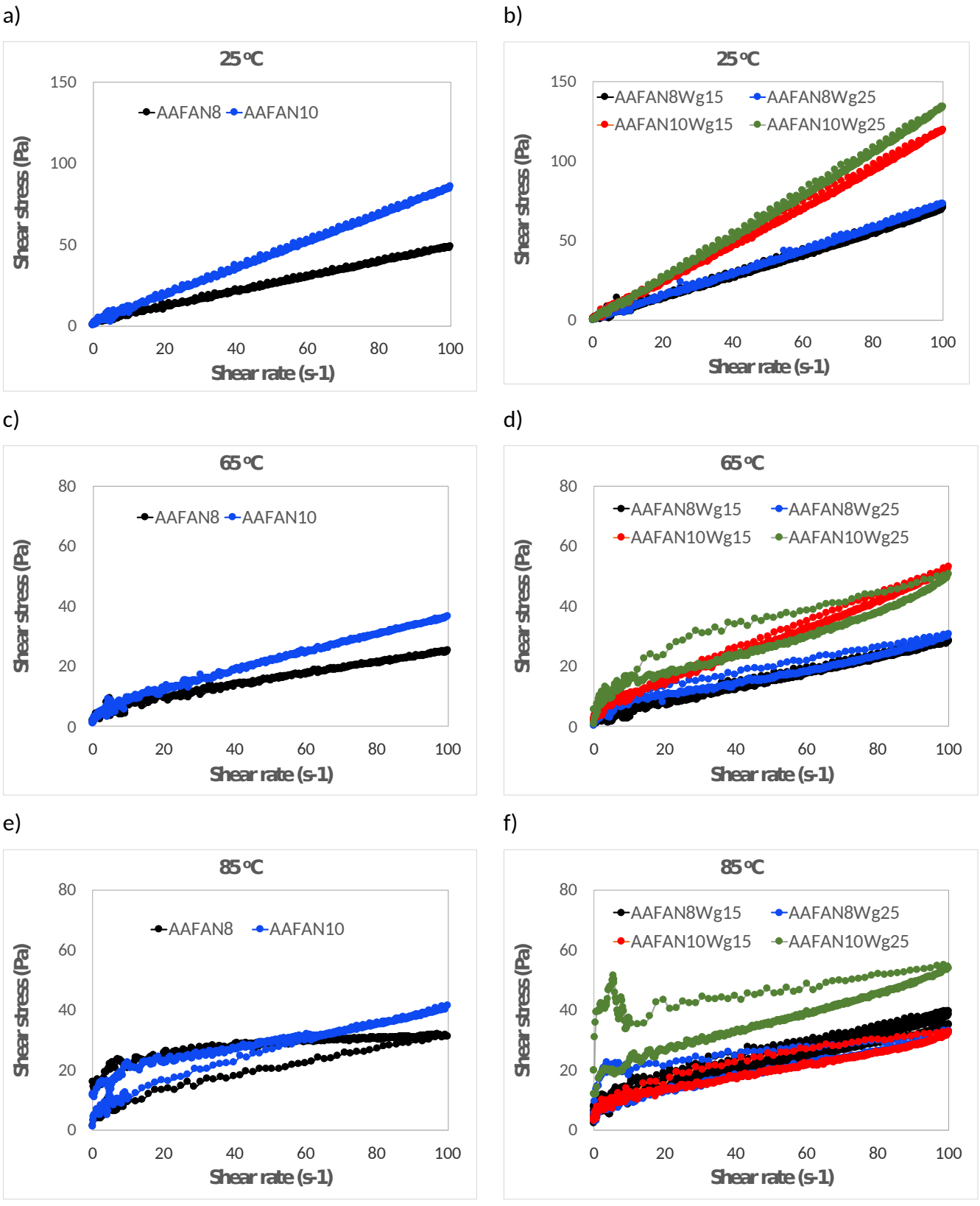

Figure 1. Hysteresis cycles for alkali-activated fly ash pastes at 25 °C, 65 °C and 85 °C

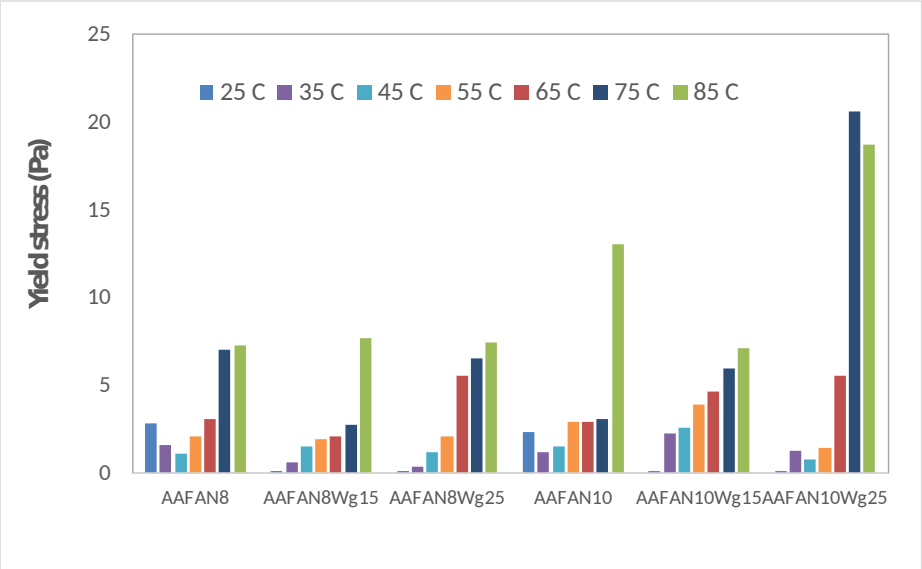

Figure 2. Yield stress of AAFA suspensions at different testing temperatures

3.2. Fluidity loss over time

The initial fluidity of the studied pastes, measured by the minislump test, was similar independently on the nature of the activating solution, its concentration and testing temperature. In particular, the spread diameter values were in the range between 110 and 140 mm.

Fluidity loss has been determined from the minislump tests by dividing the spread flow at certain time (Γ_t) by the initial spread flow (after 4 minutes of reaction, Γ_o) at the studied temperature (see Figure 3). This normalization allows a comparison of the loss of fluidity of the pastes despite the small differences of their initial spread flow. At 25 ºC, Figure 3a shows that the fluidity of AAFA pastes remains constant over the first 30 minutes of reaction with no influence of the nature and concentration of the activating solution, confirming that fly ash is not reacting at this temperature. In contrast, at 65 ºC, the nature of the activator plays a key role on the fluidity loss. While NaOH-AAFA pastes show a constant fluidity, this decreases over time for pastes activated with waterglass, being higher the flow loss as the SiO_2/Na_2O modulus of the activating solution increases. In particular, AAFAN8Wg25 and AAFAN10Wg25 hardened and did not flow after 30 minutes of reaction. Finally, at 85 ºC the flow loss occurs from the first minutes as fly ash

dissolution is enhanced at this temperature, being faster the loss of fluidity as the silica modulus and NaOH concentration increases. In particular, AAFAN10Wg25 pastes do not flow after only 18 minutes of reaction.

(a)

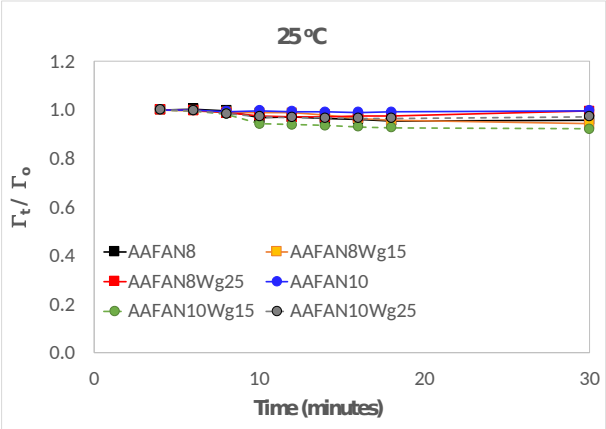

(b)

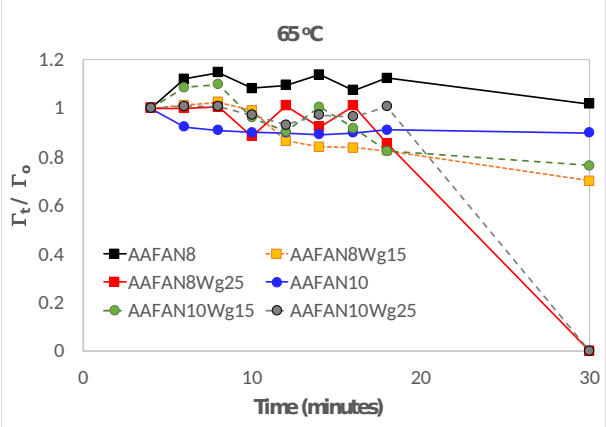

(c)

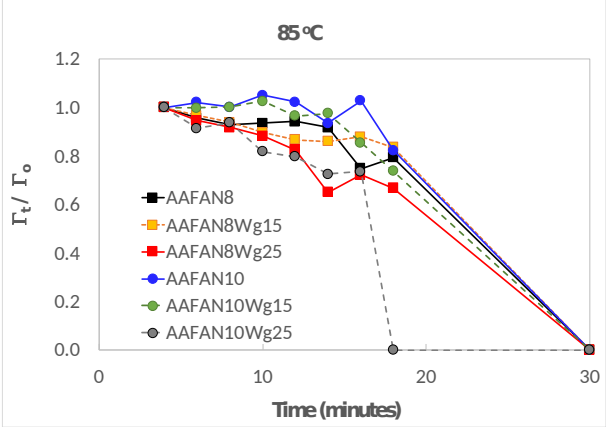

Figure 3. Fluidity loss of the AAFA pastes at (a) 25 ºC, (b) 65 ºC and (c) 85 ºC

3.3 Evolution of apparent viscosity in AAFA pastes at a constant shear rate

Figure 4 shows the evolution over time and at different temperatures of the apparent viscosity of AAFA pastes. The nature and concentration, as well as the silica modulus, of the activating solution have a clear influence on the initial apparent viscosity of the AAFA pastes. Moreover, these parameters play a key role on the shape of the viscosity-time plot due to differences in the reaction process of the fly ash.

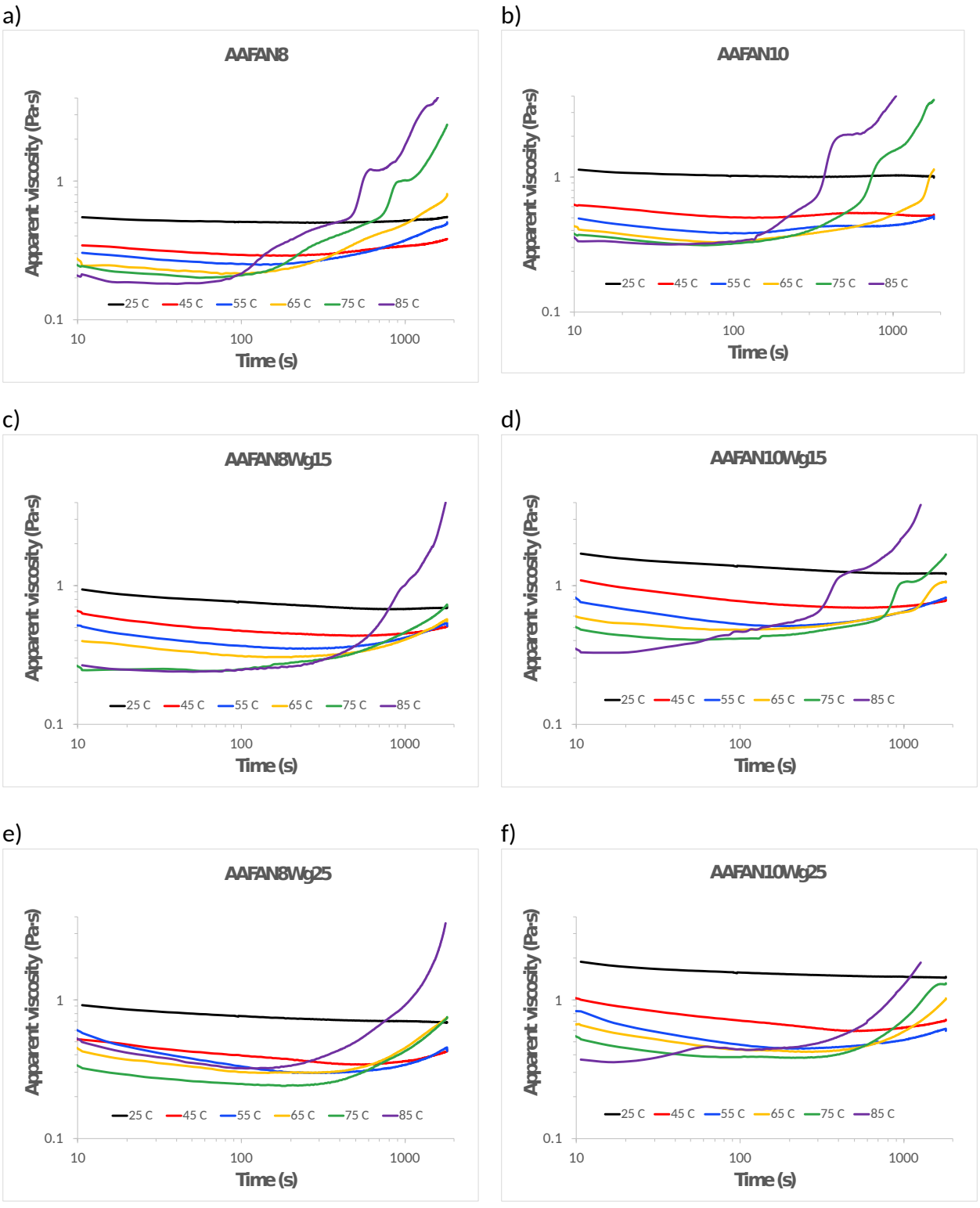

Figure 4.- Evolution over time and at different temperatures of the apparent viscosity of AAFA pastes

3.3.1. Initial apparent viscosity

An increase of the initial apparent viscosity of the AAFA pastes (after 3 minutes of mixing with alkaline solution) with the rise of the activator concentration is found at 25 ºC. This can be explained by the increase of the viscosity of the activating solution (see Table 3), due to the raise of the ion-dipole forces with the increment of the ionic concentration [18]. Furthermore, an increase of the SiO_2/Na_2O also involves a higher viscosity of the activating solution and consequently of the AAFA paste. In particular, an increase of the SiO_2/Na_2O induces both a rise of the ion-dipole but also a higher amount of colloidal Si-O-H-M complexes in solution forming aggregates of a few nanometers that increases solution viscosity [18, 30, 31].

For most of the AAFA pastes, a decrease of the initial viscosity with the rise of the temperature according to Arrhenius-Guzman equation [Eq. 3] is observed (see Figure 5). This would confirm the lack of physical or chemical reactions of the fly ash during the first minutes (around 3.5 min) of contact with the alkaline solution at all the tested temperatures. Moreover, the evolution of the initial apparent viscosity with the temperature depends on the alkali concentration of the activating solution but not on its silicate content, as it can be concluded from the overlapping of Arrhenius-Guzman plots for AAFAN8Wg15 and AAFAN8Wg25 pastes as well as for AAFAN10Wg15 and AAFAN10Wg25 pastes (see Figure 5).

$$\eta = A \cdot e^{-B/T} \qquad \text{[Eq. 3]}$$

where η is the viscosity, *A* and *B* the constants for the fluid and *T* the absolute temperature in K [32].

In contrast, the apparent viscosity of AAFAN10 pastes do not follow an Arrhenius-Guzman behaviour. In particular, a lower decrease of the viscosity with the rise of the temperature is observed above 45 °C. This could mean that above 45 °C, fly ash particles are quickly reacting after contact with the NaOH 10M solution, being this favored by the increase of the temperature and also the higher pH of this solution (see Table 3).

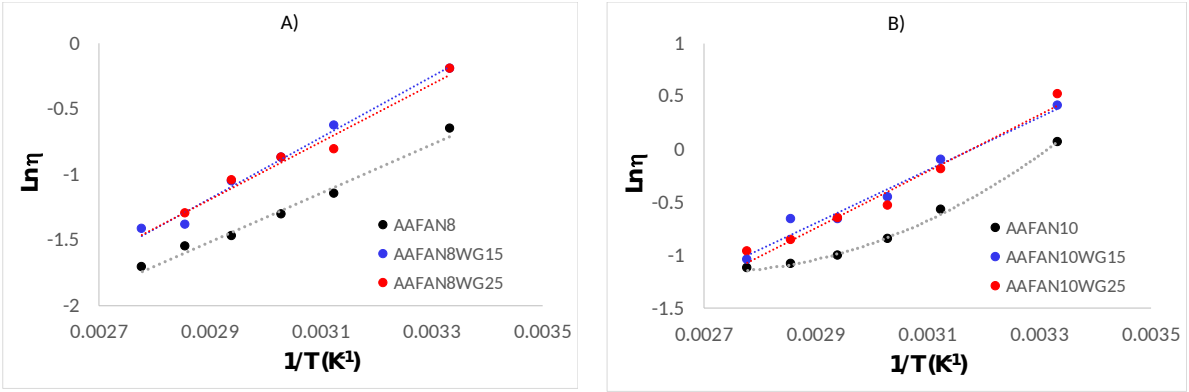

Figure 5. Evolution of the natural logarithm of the initial apparent viscosity (t = 30s) of alkali-activated pastes with the reciprocal temperature

3.3.2. Evolution of apparent viscosity over time

A constant apparent viscosity over time was found for all the AAFA pastes activated at temperatures between 25 °C and 45 °C, independently of the concentration and silica modulus of the activating solution. This would confirm the lack or slow reactivity of fly ash in this range of temperatures, as refered in the literature [23] and also shown in the minislump tests (see Figure 3). However, above 65 °C a more significant rise in apparent viscosity is observed as this is the onset of physical-chemical interactions and the

formation of the initial reaction products leading to the steady viscosity rise even as pastes were stirred during the rheological test. In particular, the increase of the temperature induces the fly ash dissolution and release of silicate and aluminate monomers to the solution. Their condensation leads to the precipitation of the first (perhaps colloidal) reaction products, precursors of an initial metastable high-aluminium aluminosilicate gel (N-A-S-H gel), known as Gel 1, with a three-dimensional structure [33, 34].

Figure 4 also shows an early appearance of the onset time as well as a higher increase of the viscosity over time with the increase of the activator concentration. This is in agreement with the higher OH^- concentration in the activating solution (see Table 3), enhacing fly ash dissolution and the formation of reaction products at lower temperatures. That concurred with reports by Fernández-Jiménez and Palomo [35], who found AAFA mortar strength to rise with increasing activator concentration due to the formation of more reaction products.

Furthermore, the onset time of viscosity increase is delayed for waterglass-activated fly ash pastes with the exception of AAFAN10Wg25 paste, that also showed the faster flow loss during the minislump tests (Figure 3). The addition of sodium silicate decreases pH and also rises the degree of polymerisation of the silicates in the activating solution [36] forming cyclic silicates that retards fly ash dissolution. Therefore, both the SiO_2/Na_2O ratio in the waterglass and the total SiO_2 and Na_2O in the solution play key roles in the reactivity of fly ash. A balance must be struck in activating solutions between the NaOH

and waterglass concentrations to maintain an optimal pH and the necessary silicate ion content to favour the formation of cementitious structures.

To gain further insights into to AAFA reaction process ocurring above 65ºC, it was determined the time needed to reach certain viscosity increase (t) as it is directly linked to the rate of reaction described by Arrhenius equation (eq. 4):

$$\frac{1}{t} = A\, e^{\frac{-E_a}{RT}} \qquad \text{(Eq. 4)}$$

where A is a pre-exponential constant, E_a is the activation energy per mole of the reaction, R is the universal gas constant and T is the absolute temperature. In Figure 6, the logarithm of the time taken to reach an increase of the apparent viscosity of 0.5 mPa·s was plotted versus the reciprocal temperature. This value of 0.5 mPa·s was chosen as it was the lower limit of the increase of the viscosity measured for the AAFA pastes over the tested time. In the case of AAFAN10Wg25 hydrated at 65 ºC, the time to reach the increase of the viscosity was extrapolated. A good linear fitting is obtained for the six pastes, where the slope is equal to E_a/R. Apparent activation energy can bring information about the underlying chemical reaction as it depends on the rate-controlling step and on the composition of the reaction products [37]. For the six AAFA pastes, the apparent activation energy is very similar (see Table 4), concluding that despite their different evolution of the viscosity over time, the underlying reaction mechanism is the same, regardless of the concentration and silica modulus of the activating solution. Furthermore, similar activation energies were also obtained by Poulesquen for NaOH- and KOH-metakaolin activated pastes [22], although kinetics of the activation process in fly ash- and metakaolin-activated systems are different. Finally, activation energies are

in between 60 and 80 kJ/mol, concluding that kinetics are surface reaction controlled [38, 39].

a) b)

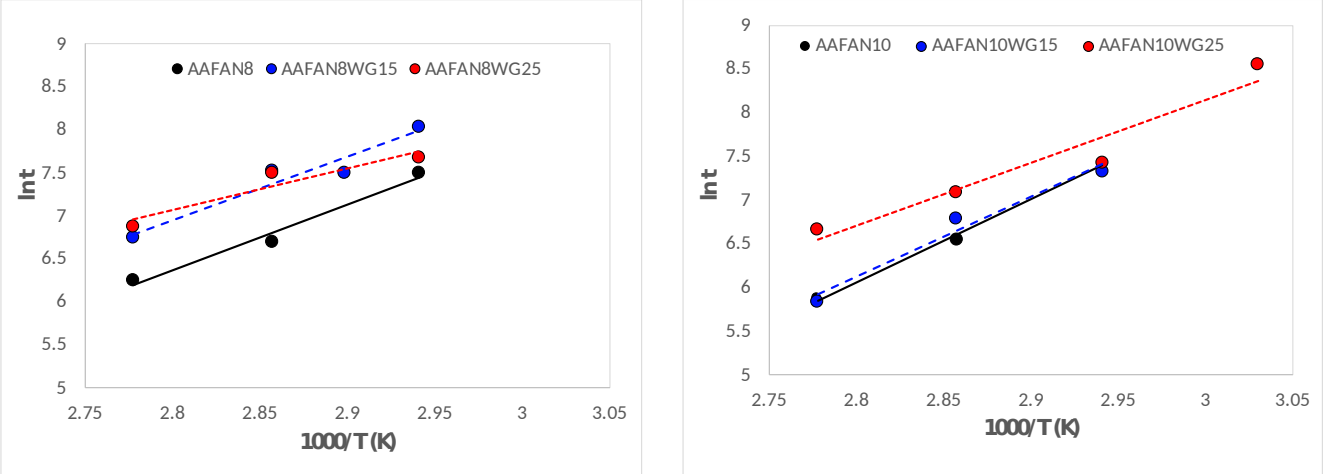

Figure 6. Arrhenius plot of the reciprocal absolute temperature versus the natural logarithm of the time needed to reach an increase of the intrinsic viscosity of 0.5 mPa·s. Linear regressions have been included.

Table 4.- Apparent activation energy of fly ash reaction

Mix	AAFAN8	AAFAN8WG15	AAFAN8WG25	AAFAN10	AAFAN10WG15	AAFAN10WG25
Activation energy (KJ/mol)	63.6	78.7	78.2	64.4	75.6	59.6

4. Conclusions

The nature and concentration of the alkaline activator and temperature play a key role on the reactivity and rheological properties of AAFA pastes. In particular:

1. At room temperature, waterglass- AAFA pastes show lower yield stress values than NaOH-AAFA. The adsorption of the silicates in the former increases the

overall negative surface charge of fly ash, increasing interparticle repulsive forces, leading to deflocculation of the particles.

2. An increase of yield stress and apparent viscosity is observed with the rise of the temperature, mainly at temperatures above 65 ºC when dissolution of fly ash and precipitation of hydration products is enhanced.

3. At all studied temperatures, an increase of the alkaline solution concentration leads to greater yield stress values due to the higher reactivity of the fly ash and the greater amount of percolated early hydration products.

4. In general, very similar activation energies were determined for all the studied alkaline-activated fly ash pastes. This involves that the underlying reaction mechanism is the same, independently on the concentration, nature and silica modulus of the activating solution.

Acknowledgements

Prof. F. Puertas thanks MINECO (Spanish Ministry) for funding BIA2013-47876-C2-1-P project. Dr. M. Palacios acknowledges Consejería de Educación e Investigación (Comunidad de Madrid) for funding the 2016-T1/AMB-1434 project in the frame of "Ayudas de Atracción de Talento Investigador". The authors wish to thank P. Rivilla for her assistance with the tests.

References

[1] G.H. Tattersall, P.F.G. Banfill, The rheology of fresh concrete, Pitman, Advanced Publishing Program, 1983.

[2] A. Yahia, S. Mantellato, R.J. Flatt, 7 - Concrete rheology: A basis for understanding chemical admixtures, in: Sci. Technol. Concr. Admix., Woodhead Publishing, 2016: pp. 97–127. doi:10.1016/B978-0-08-100693-1.00007-2.

[3] A.M. Aguirre, R.M. de Gutiérrez, Durability of reinforced concrete exposed to aggressive conditions, Mater. Constr. 63 (2013) 7–38. doi:10.3989/mc.2013.00313.
[4] J. Miranda, V. Flores-Ales, J. Barrios, Aportaciones al estudio reológico de pastas y morteros de cemento portland, Mater. Construccion. 50 (257) (2000) 47–56.
[5] M.M. Alonso, M. Palacios, F. Puertas, Compatibility between polycarboxylate-based admixtures and blended-cement pastes, Cem. Concr. Compos. 35 (2013) 151–162. doi:10.1016/j.cemconcomp.2012.08.020.
[6] M.M. Alonso, M. Palacios, F. Puertas, A.G. De la Torre, M.A.G. Aranda, Effect of polycarboxylate admixture structure on cement paste rheology, Mater. Construccion. 57 (286) (2007) 65–81.
[7] O. Burgos-Montes, M. Palacios, P. Rivilla, F. Puertas, Compatibility between superplasticizer admixtures and cements with mineral additions, Constr. Build. Mater. 31 (2012) 300–309. doi:10.1016/j.conbuildmat.2011.12.092.
[8] R. Flatt, I. Schober, 7 - Superplasticizers and the rheology of concrete, in: N. Roussel (Ed.), Underst. Rheol. Concr., Woodhead Publishing, 2012: pp. 144–208. http://www.sciencedirect.com/science/article/pii/B9780857090287500078 (accessed February 28, 2015).
[9] R. Shaughnessy, P.E. Clark, The rheological behavior of fresh cement pastes, Cem. Concr. Res. 18 (1988) 327–341. doi:10.1016/0008-8846(88)90067-1.
[10] R.J. Flatt, P. Bowen, Yield Stress of Multimodal Powder Suspensions: An Extension of the YODEL (Yield Stress mODEL), J. Am. Ceram. Soc. 90 (2007) 1038–1044. doi:10.1111/j.1551-2916.2007.01595.x.
[11] R.J. Flatt, P. Bowen, Yodel: A Yield Stress Model for Suspensions, J. Am. Ceram. Soc. 89 (2006) 1244–1256. doi:10.1111/j.1551-2916.2005.00888.x.
[12] B. González-Fonteboa, S. Seara-Paz, J. de Brito, I. González-Taboada, F. Martínez-Abella, R. Vasco-Silva, Recycled concrete with coarse recycled aggregate. An overview and analysis, Mater. Constr. 68 (2018) 151. doi:10.3989/mc.2018.13317.
[13] M.M. Alonso, R. Martínez-Gaitero, S. Gismera-Diez, F. Puertas, PCE and BNS admixture adsorption in sands with different composition and particle size distribution, Mater. Constr. 67 (2017) 121. doi:10.3989/mc.2017.08116.
[14] J.-Y. Petit, E. Wirquin, K.H. Khayat, Effect of temperature on the rheology of flowable mortars, Cem. Concr. Compos. 32 (2010) 43–53. doi:10.1016/j.cemconcomp.2009.10.003.
[15] M. Palacios, P.F.G. Banfill, F. Puertas, Rheology and Setting of Alkali-Activated Slag Pastes and Mortars: Effect of Organic Admixture, Mater. J. 105 (2008) 140–148.
[16] F. Puertas, C. Varga, M.M. Alonso, Rheology of alkali-activated slag pastes. Effect of the nature and concentration of the activating solution, Cem. Concr. Compos. 53 (2014) 279–288. doi:10.1016/j.cemconcomp.2014.07.012.
[17] M. Romagnoli, C. Leonelli, E. Kamse, M. Lassinantti Gualtieri, Rheology of geopolymer by DOE approach, Constr. Build. Mater. 36 (2012) 251–258. doi:10.1016/j.conbuildmat.2012.04.122.
[18] K. Vance, A. Dakhane, G. Sant, N. Neithalath, Observations on the rheological response of alkali activated fly ash suspensions: the role of activator type and concentration, Rheol. Acta. 53 (2014) 843–855. doi:10.1007/s00397-014-0793-z.
[19] M. Torres-Carrasco, C. Rodríguez-Puertas, M. del M. Alonso, F. Puertas, Alkali activated slag cements using waste glass as alternative activators. Rheological behaviour, Bol. Soc. Esp. Cerámica Vidr. 54 (2015) 45–57. doi:10.1016/j.bsecv.2015.03.004.

[20] A. Favier, G. Habert, N. Roussel, J.-B. d'Espinose de Lacaillerie, A multinuclear static NMR study of geopolymerisation, Cem. Concr. Res. 75 (2015) 104–109. doi:10.1016/j.cemconres.2015.03.003.
[21] P. Duxson, A. Fernández-Jiménez, J.L. Provis, G.C. Lukey, A. Palomo, J.S.J. van Deventer, Geopolymer technology: the current state of the art, J. Mater. Sci. 42 (2007) 2917–2933. doi:10.1007/s10853-006-0637-z.
[22] A. Poulesquen, F. Frizon, D. Lambertin, Rheological behavior of alkali-activated metakaolin during geopolymerization, J. Non-Cryst. Solids. 357 (2011) 3565–3571. doi:10.1016/j.jnoncrysol.2011.07.013.
[23] A. Palomo, P.F.G. Banfill, A. Fernández-Jiménez, D.S. Swift, Properties of alkali-activated fly ashes determined from rheological measurements, Adv. Cem. Res. 17 (2005) 143–151. doi:10.1680/adcr.2005.17.4.143.
[24] M. Palacios, H. Kazemi-Kamyab, S. Mantellato, P. Bowen, Laser diffraction and gas adsorption techniques, in: Pract. Guide Microstruct. Anal. Cem. Mater., 2015.
[25] C. Ruiz-Santaquiteria, M. Torres-Carrasco, M.M. Alonso, F. Puertas, Valorización de residuos vítreos en la elaboración de morteros alcalinos. Workshop on Environmental Impact of Buildings (WEIB), 2013.
[26] N. Roussel, Steady and transient flow behaviour of fresh cement pastes, Cem. Concr. Res. 35 (2005) 1656–1664. doi:10.1016/j.cemconres.2004.08.001.
[27] D. Lowke Peter J.M. |Bittnar,Zdenek|Nemecek,Jiri|Smilauer,V.|Zeman,J., Interparticle Forces and Rheology of Cement Based Suspensions, (2009) 295–301.
[28] G. Landrou, C. Brumaud, F. Winnefeld, R.J. Flatt, G. Habert, Lime as an Anti-Plasticizer for Self-Compacting Clay Concrete, Materials. 9 (2016) 330. doi:10.3390/ma9050330.
[29] A. Favier, J. Hot, G. Habert, N. Roussel, J.-B. d'Espinose de Lacaillerie, Flow properties of MK-based geopolymer pastes. A comparative study with standard Portland cement pastes, Soft Matter. 10 (2014) 1134–1141. doi:10.1039/C3SM51889B.
[30] J.F. Stebbins, I. Farnan, X. Xue, The structure and dynamics of alkali silicate liquids: A view from NMR spectroscopy, Chem. Geol. 96 (1992) 371–385. doi:10.1016/0009-2541(92)90066-E.
[31] M.T. Tognonvi, D. Massiot, A. Lecomte, S. Rossignol, J.-P. Bonnet, Identification of solvated species present in concentrated and dilute sodium silicate solutions by combined 29Si NMR and SAXS studies, J. Colloid Interface Sci. 352 (2010) 309–315. doi:10.1016/j.jcis.2010.09.018.
[32] R. Moreno, Reología de las suspensiones cerámicas, 2005.
[33] A. Palomo, P. Krivenko, I. Garcia-Lodeiro, E. Kavalerova, O. Maltseva, A. Fernández-Jiménez, A review on alkaline activation: new analytical perspectives, Mater. Constr. 64 (2014) 022.
[34] A. Fernández-Jiménez, A. Palomo, I. Sobrados, J. Sanz, The role played by the reactive alumina content in the alkaline activation of fly ashes, Microporous Mesoporous Mater. 91 (2006) 111–119. doi:10.1016/j.micromeso.2005.11.015.
[35] A. Fernández-Jiménez, A. Palomo, Composition and microstructure of alkali activated fly ash binder: Effect of the activator, Cem. Concr. Res. 35 (2005) 1984–1992. doi:10.1016/j.cemconres.2005.03.003.
[36] M. Criado, A. Palomo, A. Fernández-Jiménez, Alkali activation of fly ashes. Part 1: Effect of curing conditions on the carbonation of the reaction products, Fuel. 84 (2005) 2048–2054. doi:10.1016/j.fuel.2005.03.030.
[37] J.J. Thomas, The Instantaneous Apparent Activation Energy of Cement Hydration Measured Using a Novel Calorimetry-Based Method, J. Am. Ceram. Soc. 95 (n.d.) 3291–3296. doi:10.1111/j.1551-2916.2012.05396.x.

[38] P. Juilland, E. Gallucci, Morpho-topological investigation of the mechanisms and kinetic regimes of alite dissolution, Cem. Concr. Res. 76 (2015) 180–191. doi:10.1016/j.cemconres.2015.06.001.
[39] A.C. Lasaga, Rate laws of chemical reactions, in P.H. Ribbe (Ed), Reviews in mineralogy - kinetcis of geochemical processes- BookCrafter Inc., 1981.